# Systematic variations in recurrence interval and moment of repeating aftershocks

Zhigang Peng,[1] John E. Vidale,[1] Chris Marone,[2] and Allan Rubin[3]

Received 4 February 2005; revised 10 June 2005; accepted 6 July 2005; published 2 August 2005.

[1] The recurrence intervals for 194 repeating clusters on the Calaveras fault follow a power-law decay relation with elapsed time after the 1984 M6.2 Morgan Hill, California, mainshock. The decay rates of repeating aftershocks in the immediate vicinity of a high-slip patch that failed during the mainshock systematically exceed those that are farther away. The trend between relative moment and recurrence interval, which is a measure of the fault-healing rate, varies systematically with depth and changes from negative to positive value as the distance between the repeating aftershock and the mainshock slip patch increases. We speculate that high strain rate in the early postseismic period may cause transient embrittlement and strengthening of the deep repeating clusters in the areas adjacent to the mainshock slip patch, resulting in large moments that decrease with time as the strain rate diminishes. Our observations suggest that systematic behavior of repeating aftershocks reflect variations in the fault zone rheology.
**Citation:** Peng, Z., J. E. Vidale, C. Marone, and A. Rubin (2005), Systematic variations in recurrence interval and moment of repeating aftershocks, *Geophys. Res. Lett.*, *32*, L15301, doi:10.1029/2005GL022626.

## 1. Introduction

[2] Laboratory studies predict that earthquake fault zones regain strength (heal) during the inter-seismic period [*Dieterich*, 1972; *Johnson*, 1981]. Recently, direct observations of shallow fault healing after major earthquakes in California have been documented [*Vidale and Li*, 2003]. A clear understanding of fault healing has important implications for many aspects of earthquake physics, including long-term evolution of faults, hazard mitigation, and the mode of dynamic rupture propagation.

[3] One effective way of measuring fault-healing rate is to examine behaviors of small repeating earthquakes [e.g., *Vidale et al.*, 1994; *Marone et al.*, 1995]. Recent developments in earthquake relocation [e.g., *Waldhauser and Ellsworth*, 2000; *Schaff et al.*, 2002] have significantly reduced relative location errors, and led to identification of many sets of repeating earthquakes [e.g., *Schaff et al.*, 1998; *Rubin*, 2002]. In this study, we analyze 194 sequences of repeating earthquakes in the aftershock zone of the 1984 Morgan Hill earthquake along the Calaveras fault (Figure 1a). We first examine the dependence of recurrence interval on elapsed time since the mainshock, and the relation between relative moment and recurrence interval for these repeating clusters. We then compare the relations for different clusters with the slip distribution of the Morgan Hill mainshock and discuss possible mechanisms that explain our observations.

## 2. Repeating Earthquakes

[4] A total of 194 repeating clusters are identified among 3672 relocated events in the aftershock zone of the Morgan Hill earthquake (Figure 1b). Among them, 92 clusters have been identified in *Rubin* [2002]. The remaining 102 clusters are identified by visual inspection based on the relocation after time-dependent station corrections [*Rubin*, 2002]. Our selection criteria are: magnitude difference smaller than 1.5, clear spatial separation from nearby earthquakes (not within their source areas assuming a 3-MPa stress drop), the near complete overlapping of source areas (>50%), and the absence of any obvious short-term triggering between events of the same cluster. The number of events in each repeating cluster ranges from 3 to 23, resulting in a total of 1467 events that classify as repeating earthquakes. The mean magnitude for these repeating earthquakes is ~1.25, corresponding to a radius of ~25 m for a 3-MPa stress drop. This rupture size is much larger than the location error, which is a few meters for repeating earthquakes [*Rubin*, 2002], suggesting that these earthquakes repeatedly rupture the same fault patches.

## 3. Recurrence Interval Versus Elapsed Time

[5] The ~1500 earthquakes within the 194 repeating clusters are aftershocks of the Morgan Hill earthquake, and follow a general pattern of decaying aftershock rate. Figure 2a shows the time intervals between consecutive repeating events, *Tr*, for two example clusters (47 and 54) as a function of average elapsed time *t* after the mainshock. The recurrence intervals *Tr* of both clusters appear to follow a power law relation with *t*. A least-square, best-fit power law ($Tr \sim t^p$) is shown, where the exponent *p* is equivalent to the slope in Figure 2a. For each cluster, we also calculate the logarithm of maximum minus minimum recurrence interval *Tr*, or the recurrence interval range (RIR). Larger (smaller) RIR value means larger (smaller) change in *Tr* over the time of the observation.

[6] Figure 2b presents the spatial distribution of *p* and RIR values for the 194 clusters. Among them, 104 clusters with along-strike distance $0 \leq x \leq 10.5$ km and depth $z \geq 4$ km (bounded by the dashed line in Figure 2b) have relatively large *p* (0.65 ± 0.25) and RIR (1.33 ± 0.60) values, while the remaining 90 clusters have relatively small *p* (0.28 ± 0.37) and RIR (0.68 ± 0.36) values.

[1]Department of Earth and Space Sciences, University of California, Los Angeles, California, USA.
[2]Department of Geosciences, Pennsylvania State University, University Park, Pennsylvania, USA.
[3]Department of Geosciences, Princeton University, Princeton, New Jersey, USA.


0094-8276/05/2005GL022626$05.00

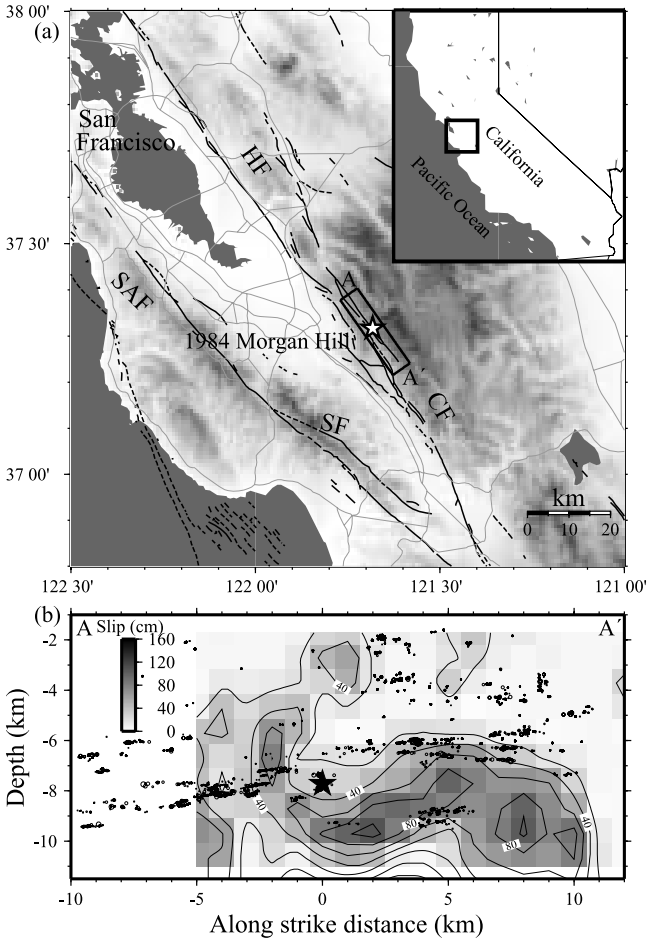


**Figure 1.** (a) Location of the Calaveras fault in California. The box corresponds to our study area. Dark and gray lines denote nearby faults and roads, respectively. Shaded background indicates topography with white being low and dark being high. The star marks the epicentral location of the 1984 Morgan Hill mainshock. The inset shows the map of California. SAF, San Andreas fault; SF, Sargent fault; CF, Calaveras fault; HF, Hayward fault. (b) Hypocenters of 3672 relocated earthquakes [*Rubin*, 2002] along the cross-section AA′ in (a). Shaded background denotes the slip distribution of the Morgan Hill mainshock [*Beroza and Spudich*, 1988].

[7] Figure 2b also shows a slip distribution of the Morgan Hill mainshock obtained from waveform modeling of near-fault strong motion data [*Beroza and Spudich*, 1988]. Although the spatial resolution in the slip model is probably not well constrained, it is clear that an area of high slip during the mainshock with $0 \leq x \leq 10$ km and $6 \leq z \leq 10$ km, is surrounded by repeating clusters with relatively large $p$ and RIR values. We speculate that regions in the immediate vicinity of the mainshock slip patch were highly loaded and began to creep rapidly after the mainshock. As the fault creeps, it concentrates shear stress on many small patches, which fail in repeated earthquakes. The rate of repeated failure in the highly stressed region is expected to decay rapidly with time as the stress relaxes, resulting in relatively large RIR and $p$ values. In comparison, the mainshock stressing is smaller for clusters at relatively shallow depth and far from the high slip patch of the mainshock. Thus, the RIR and $p$ values for these repeating clusters are expected to be small.

## 4. Moment Versus Recurrence Interval

[8] The relation between relative seismic moment ($Mo$) and $Tr$ for repeating clusters is a proxy measure of the rate of fault healing. $Mo$ is calculated from the coda magnitude for each event in the NCSN catalog using a moment-magnitude relation of *Abercrombie* [1996], and then normalized by the mean of each cluster. Figure 3a shows $Mo$ against $Tr$ for two examples. Cluster 19 exhibits increasing $Mo$ with increasing $Tr$ and cluster 47 shows the

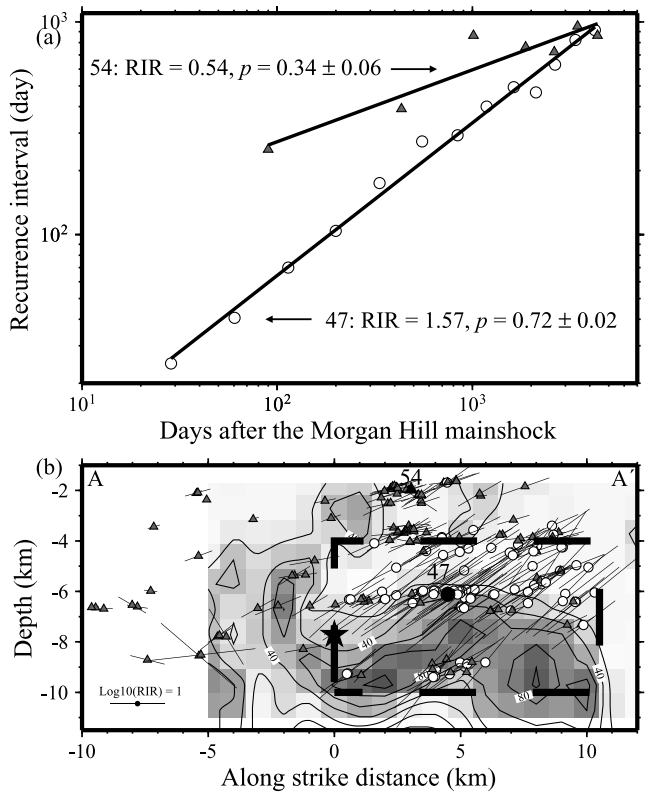


**Figure 2.** (a) The recurrence interval ($Tr$) as a function of the elapsed time ($t$) after the Morgan Hill mainshock. The circles and triangles denote results for cluster 47 and 54, respectively. The centroid locations of these two clusters are marked in (b). The lines give the least square fit using the power law equation $Tr \sim t^p$. The error is computed from the formal standard errors of the line fit. (b) The exponent $p$ (lines) for the best-fit power-law curve between $Tr$ and $t$ superimposed on the centroid location for each of the 194 clusters. The line is oriented parallel to the exponent $p$ using the axes of panel (a), and its length is scaled by the logarithm range of the recurrence intervals (RIR). The circles denotes 79 clusters that satisfy the following two criteria: RIR $\geq$ 1.0 and the correlation coefficient (CC) between the log($Tr$) and log($t$) $\geq$ 0.7. This region is bounded approximately by the dashed line. The triangles denote clusters that do not satisfy the above criteria. See color version of this figure in the HTML.

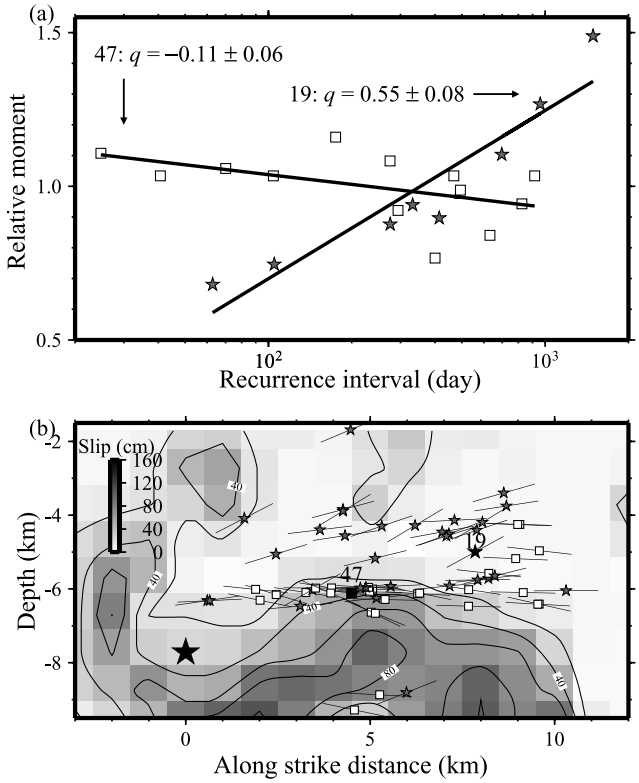


**Figure 3.** (a) Relative moment (*Mo*) plotted against recurrence interval (*Tr*) for cluster 19 (stars) and 47 (squares). The line denotes the least-square fit to the data using the relation $Mo \sim q \log_{10}(Tr)$. The centroid locations of these two clusters are marked in (b). (b) The moment trends, or *q* values (lines) superimposed on the centroid locations of 55 clusters that satisfy the two criteria in Figure 2 and have a standard error of fit of no more than 0.2. The squares and stars mark the locations of the clusters with negative and positive changing trend, respectively. See color version of this figure in the HTML.

opposite trend. We fit the data by least-squares using a relation $Mo \sim q \log_{10}(Tr)$, where *q* is the measure of fault-healing rate, and is equivalent to the slope in Figure 3a.

[9] To better constrain the relation between *Mo* and *Tr*, a wide range of *Tr* (large RIR) is needed. Other factors, such as the occurrence of a large aftershock nearby, may affect the rupture properties and *Tr* of repeating clusters. A high correlation coefficient (CC) between log(*Tr*) and log(*t*) suggests a simple relationship of increasing *Tr* with increasing *t* after the Morgan Hill mainshock, and an absence of other complexities in *Tr*. Since we are mostly interested in variations of these properties induced by transient creep due to the mainshock, we select 79 clusters (red circles in Figure 2b) that have relatively large RIR ($\geq$1.0) and high CC ($\geq$0.7) between log(*Tr*) and log(*t*) for further analysis. In addition, we discard the results for 24 clusters that do not show a simple relationship between *Mo* and *Tr* (standard error of the fit more than 0.2).

[10] The *q* values for the resulting 55 clusters are plotted on top of their centroid locations in Figure 3b. It is clear that most of the shallow clusters ($z \leq 5.5$ km) have large and positive *q* values. In comparison, clusters at $z \geq 5.5$ km that are in the immediate vicinity of the mainshock slip patch have a mixture of positive and negative *q* values. Since only clusters with along-strike distance of $0 \leq x \leq 10$ km are selected, we use their hypocentral depths (*z*) to approximate their distance to the mainshock slip patch. Figure 4 shows the variation of *q* values for the 55 clusters with their hypocentral depths. The *q* values appear to decrease with increasing depths (decreasing distances to the mainshock slip patch), although this trend is weak (with a correlation coefficient of 0.46). We also estimate the *q* values for the CA1 and CA2 clusters that are located at the southern end of the Morgan Hill rupture zone, which were analyzed previously by *Vidale et al.* [1994] and *Marone et al.* [1995]. The obtained results are compatible with other *q* values.

## 5. Interpretation

[11] Frictional healing (as evidenced by increasing static friction during quasi-stationary contact in laboratory experiments) is considered the most likely mechanism of interseismic fault strengthening [*Dieterich*, 1972; *Johnson*, 1981]. Simulations with rate and state-variable equations [*Gu and Wong*, 1991; *Marone*, 1998; *Beeler et al.*, 2001] and laboratory experiments [*Karner and Marone*, 2000] have shown that variations in the failure strength (or stress drop) depends on the coupled effects between loading rate variation and change in frictional state, which is roughly equivalent to asperity contact area. However, our data show that fault zone restrengthening, in the context of the seismic cycle, is more complex than previously thought. On the one hand, the observation of positive moment trends with *Tr* (*q* values) for most shallow clusters with $z \leq 5.5$ km is

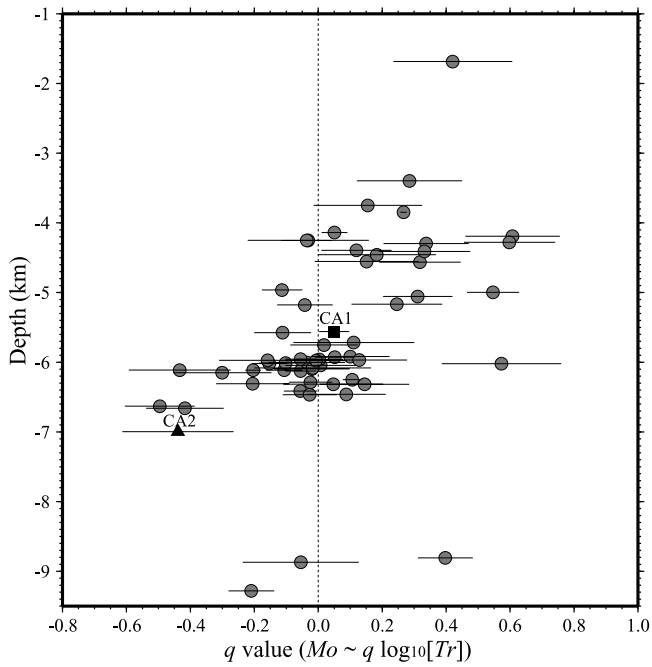


**Figure 4.** The moment trends (*q* values) with recurrence interval plotted against their average hypocentral depths for the 55 clusters. The square and triangle denote the results for CA1 and CA2 repeating clusters used by *Vidale et al.* [1994] and *Marone et al.* [1995].

consistent with previous laboratory studies. However, some deep repeating clusters show negative moment trends, which would imply decreasing frictional yield strength and/or stress drop with increasing earthquake recurrence interval. Laboratory experiments have documented such time-dependent frictional weakening under special conditions [e.g., *Karner and Marone*, 2001], however, it is not clear how those results would apply in the present case.

[12] One possible explanation involves rapid postseismic creep in areas directly adjacent to the mainshock slip patch. These areas will creep in response to the stress step from the mainshock, and then relax rapidly with time. High strain rates right after the mainshock may cause transient embrittlement in areas directly adjacent to the mainshock, resulting in an increase in *M*o for the deep repeating clusters in the early postseismic period. As the strain rate decreases with time, these areas would return to a neutrally-stable frictional behavior with concomitant reduction in stress drop. The ensuing reduction of *M*o due to diminishing strain rate after the mainshock may overwhelm the increased strength due to fault healing, resulting in a near-constant or even decreasing *M*o with increasing *Tr*.

[13] Laboratory experiments have shown positive dependence of the fault strength on the strain rate [*Kato et al.*, 1992; *Blanpied et al.*, 1995]. A time-dependent variation of strain rate may result in a temporary deepening of the seismic-aseismic transition zone right after the mainshock. Thus, repeating events near the seismic-aseismic transition zone may disappear over time. Indeed, we found that for the 13 deepest repeating clusters within the region $3 \leq x \leq 6$ km and $8.5 \leq z \leq 9.5$ km, 7 clusters with $z \geq 9.0$ km only exist in the immediate postseismic period up to year 1986, while the 6 shallower clusters persist much longer. Similar results are obtained for the same region using a different relocated catalog [*Schaff et al.*, 2002], consistent with this interpretation. The result of a weak dependence of moment trends ($q$ values) on depth is also compatible with the laboratory studies showing decreasing fault-healing rates with increasing temperature [*Karner et al.*, 1997].

## 6. Conclusion

[14] We found that *Tr* of 194 repeating aftershocks follow a power-law relation with elapsed time $t$ after the Morgan Hill mainshock. This result is compatible with the $1/t$ decay in frequency of repeating earthquakes in the aftershock zone of the 1989 Loma Prieta earthquake [*Schaff et al.*, 1998]. The decay rates ($p$ value) for many repeating clusters are less than 1, and vary systematically with depth and along strike. In addition, we measured the fault-healing rate ($q$ value) from the trend in *M*o with increasing *Tr* for 55 clusters. Our results indicate positive healing rates for shallow clusters ($z \leq 5.5$ km) and near constant or negative healing rates for deep clusters ($z \geq 5.5$ km). The clusters that have large $p$ values and small or negative healing rates are close to a large slip patch that broke during the mainshock. We speculate that a higher strain rate right after the mainshock may cause transient embrittlement and strengthening of fault patches in the areas adjacent to the mainshock, resulting in higher moment for shorter recurrence interval. In these areas, the combined effects of diminishing strain rate and fault healing may result in near constant or negative moment trend with increasing recurrence interval. Our results indicate that systematic behavior of repeating aftershocks can be used to infer variations in the fault zone rheology and provide constraints on the slip distribution of the mainshock.

[15] **Acknowledgments.** We are grateful to Yehuda Ben-Zion, Gregory Beroza, Stephen Karner, and Justin Rubinstein for helpful discussions. The manuscript benefited from critical comments by the reviewers Nick Beeler and David Schaff. We thank Martin Mai for making the finite source slip distribution of the Morgan Hill mainshock available online.

## References

Abercrombie, R. E. (1996), The magnitude-frequency distribution of earthquakes recorded with deep seismometers at Cajon Pass, southern California, *Tectonophysics*, *261*, 1–7.

Beeler, N. M., S. H. Hickman, and T.-F. Wong (2001), Earthquake stress drop and laboratory-inferred interseismic strength recovery, *J. Geophys. Res.*, *106*, 30,701–30,713.

Beroza, G. C., and P. Spudich (1988), Linearized inversion for fault rupture behavior: Application to the 1984, Morgan Hill, California, earthquake, *J. Geophys. Res.*, *93*, 6275–6296.

Blanpied, M. L., D. A. Lockner, and J. D. Byerlee (1995), Frictional slip of granite at hydrothermal conditions, *J. Geophys. Res.*, *100*, 13,045–13,064.

Dieterich, J. H. (1972), Time-dependent friction in rocks, *J. Geophys. Res.*, *77*, 3690–3697.

Gu, Y., and T.-F. Wong (1991), Effects of loading velocity, stiffness and inertia on the dynamics of a single degree of freedom spring-slider system, *J. Geophys. Res.*, *96*, 21,677–21,691.

Johnson, T. (1981), Time dependent friction of granite: Implications for precursory slip on faults, *J. Geophys. Res.*, *86*, 6017–6028.

Karner, S. L., and C. Marone (2000), Effects of loading rate and normal stress on stress drop and stick-slip recurrence interval, in *Geocomplexity and the Physics of Earthquakes*, *Geophys. Monogr. Ser.*, vol. 120, edited by J. B. Rundle, D. Turcotte, and W. Klein, pp. 187–198, AGU, Washington, D. C.

Karner, S. L., and C. Marone (2001), Frictional restrengthening in simulated fault gouge: Effect of shear load perturbations, *J. Geophys. Res.*, *106*, 19,319–19,337.

Karner, S. L., C. Marone, and B. Evans (1997), Laboratory study of fault healing and lithification in simulated fault gouge under hydrothermal conditions, *Tectonophysics*, *277*, 41–55.

Kato, N., K. Yamamoto, H. Yamamoto, and T. Hirasawa (1992), Strain-rate effect on frictional strength and the slip nucleation process, *Tectonophysics*, *211*, 269–282.

Marone, C. (1998), The effect of loading rate on static friction and the rate of fault healing during the earthquake cycle, *Nature*, *391*, 69–72.

Marone, C., J. E. Vidale, and W. L. Ellsworth (1995), Fault healing inferred from time dependent variations in source properties of repeating earthquakes, *Geophys. Res. Lett.*, *22*, 3095–3098.

Rubin, A. M. (2002), Using repeating earthquakes to correct high-precision earthquake catalogs for time-dependent station delays, *Bull. Seismol. Soc. Am.*, *92*, 1647–1659.

Schaff, D. P., G. C. Beroza, and B. E. Shaw (1998), Postseismic response of repeating aftershocks, *Geophys. Res. Lett.*, *25*, 4549–4552.

Schaff, D. P., G. H. R. Bokelmann, G. C. Beroza, F. Waldhauser, and W. L. Ellsworth (2002), High resolution image of Calaveras Fault seismicity, *J. Geophys. Res.*, *107*(B9), 2186, doi:10.1029/2001JB000633.

Waldhauser, F., and W. L. Ellsworth (2000), A double-difference earthquake location algorithm: Method and application to the northern Hayward Fault, California, *Bull. Seismol. Soc. Am.*, *90*, 1353–1368.

Vidale, J. E., and Y.-G. Li (2003), Damage to the shallow Landers fault from the nearby Hector Mine earthquake, *Nature*, *421*, 524–526.

Vidale, J. E., W. L. Ellsworth, A. Cole, and C. Marone (1994), Variations in rupture process with recurrence interval in a repeated small earthquake, *Nature*, *368*, 624–626.

C. Marone, Department of Geosciences, Pennsylvania State University, University Park, PA 16802, USA.

Z. Peng and J. E. Vidale, Department of Earth and Space Sciences, University of California, Los Angeles, CA 90095-1567, USA. (zpeng@moho.ess.ucla.edu)

A. Rubin, Department of Geosciences, Princeton University, Princeton, NJ 08554-1003, USA.